

## A THERMAL STUDY OF HYDRATED LANTHANIDE HEPTAFLUOROBUTYRATES\*

K. W. RILLINGS\*\* AND J. E. ROBERTS

*Department of Chemistry, University of Massachusetts, Amherst, MA 01002 (U.S.A.)*

### ABSTRACT

Several hydrated lanthanide salts of heptafluorobutyric acid have been prepared and characterized.

Hydration studies have shown the compounds to exist in various hydration states across the series. Powder X-ray diffraction studies support the existence of variable hydration states in that three distinct crystalline forms exist. Infrared analysis revealed two types of structures to be present. Upon dehydration of the lighter rare earth hydrates to intermediate dihydrates, all of the compounds showed similar structures. Decomposition was found to be exothermic. The volatile decomposition products were identified by infrared analysis and found to consist of CO, CO<sub>2</sub>, CF<sub>3</sub>CF<sub>2</sub>COF and CF<sub>3</sub>CF<sub>2</sub>CF<sub>2</sub>COF. The amounts of each gas were found to be dependent on the decomposition temperature. The non-volatile decomposition products were identified by powder X-ray diffraction and found to consist of LnF<sub>3</sub>, LnOF and Ln<sub>2</sub>O<sub>3</sub>.

### INTRODUCTION

The thermal decomposition of lanthanide trifluoroacetates and pentafluoropropionates has previously been reported<sup>1, 2</sup>. The trends revealed in the thermal decomposition of these salts made it of interest to extend the study to salts of heptafluorobutyric acid.

To complete the study of this series, the present investigation is concerned with a thermal study of Pr, Sm, Eu, Gd, Ho, Er and Yb heptafluorobutyrate. A comparison has been made regarding hydration states, modes of dehydration and volatile and non-volatile decomposition products. Powder X-ray diffraction and infrared analyses have been used to identify and support the thermal findings.

\* This paper is based on a portion of the Ph.D. dissertation of K. W. Rillings, University of Massachusetts, Amherst, MA, 1973.

\*\* Present address: Springfield Technical Community College Springfield, Ma 01105, (U.S.A.).

## EXPERIMENTAL

*Reagents*

Heptafluorobutyric acid (Matheson, Coleman and Bell) was fractionally distilled twice over a column packed with glass helices. The portion of the distillate collected was that which distilled over at a temperature range of 119–121 °C. Titration of the distillate with sodium hydroxide revealed a minimum purity of 99.6%.

Lanthanide oxides, A. D. McKay or from private stock, were of 99.9% purity or better. Prior to use, the oxides were freshly ignited at 800 °C in platinum crucibles.

*Preparation of salts*

Excess lanthanide oxide was added to a 50% aqueous solution of heptafluorobutyric acid and refluxed. The lighter oxides required less time (approximately 1 h) to go into solution, while heavier oxides generally required 2 to 3 h. The solution was allowed to cool and stand for several hours after which the excess oxide was removed by filtration. Attempts to crystallize the salts by slow evaporation were unsuccessful; therefore, the solution was brought to dryness over a steam bath. The resulting compounds were dissolved in reagent grade diethyl ether (approximately 5% H<sub>2</sub>O) and filtered. Spectroscopic grade carbon tetrachloride was added until the cloud point was reached. Diethyl ether was slowly added until the solution became clear. Upon standing, the compounds crystallized from the solvent pair as long needles. The crystals were separated by filtration and air dried.

Compounds for study were prepared by drying over magnesium perchlorate under vacuum for several days. Rehydration in a hygostat over deliquescent sodium bromide (58% relative humidity) yielded the hydrates shown in Table I.

The lanthanide content of the respective compounds was determined by precipitation with oxalic acid and weighed as the oxide. Carbon analyses were provided by the Office of Research Services, University of Massachusetts, Amherst. In all cases the results of the metal and carbon analyses agreed to better than 2% of the theoretical

TABLE I

HYDRATION DATA AT 58% HUMIDITY

<i>Compound</i>	<i>Calc. molecular weight</i>	<i>Exp. molecular weight</i>
Pr(C <sub>4</sub> F <sub>7</sub> O <sub>2</sub> ) <sub>3</sub> · 4H <sub>2</sub> O	852.2	851.9
Sm(C <sub>4</sub> F <sub>7</sub> O <sub>2</sub> ) <sub>3</sub> · 3.5H <sub>2</sub> O	854.5	852.4
Eu(C <sub>4</sub> F <sub>7</sub> O <sub>2</sub> ) <sub>3</sub> · 3.5H <sub>2</sub> O	853.0	854.0
Gd(C <sub>4</sub> F <sub>7</sub> O <sub>2</sub> ) <sub>3</sub> · 3H <sub>2</sub> O	851.0	850.3
Ho(C <sub>4</sub> F <sub>7</sub> O <sub>2</sub> ) <sub>3</sub> · 2H <sub>2</sub> O	842.5	840.0
Er(C <sub>4</sub> F <sub>7</sub> O <sub>2</sub> ) <sub>3</sub> · 2H <sub>2</sub> O	843.0	842.3
Yb(C <sub>4</sub> F <sub>7</sub> O <sub>2</sub> ) <sub>3</sub> · 2H <sub>2</sub> O	848.0	848.0

TABLE 2

POWDER X-RAY DIFFRACTION DATA OF HYDRATED SALTS

Rel. intensity	$d(\text{Å})$		
	$\text{Pr}(\text{C}_4\text{F}_7\text{O}_2)_3 \cdot 4\text{H}_2\text{O}$	$\text{Sm}(\text{C}_4\text{F}_7\text{O}_2)_3 \cdot 3.5\text{H}_2\text{O}$	$\text{Eu}(\text{C}_4\text{F}_7\text{O}_2)_3 \cdot 3.5\text{H}_2\text{O}$
vs	14.81	14.76	14.85
s	7.97	8.00	8.00
m	7.53	7.47	7.46
m	6.61	6.68	6.67
m	5.90	5.83	5.83
m	5.09	5.14	5.13
m	5.02	4.97	4.97
m	4.94	4.91	4.89
s	4.59	4.53	4.53
vs	4.34	4.30	4.29
m	3.78	3.75	3.75
m	3.02	3.04	3.04
m	2.51	2.55	2.55

Rel. intensity	$d(\text{Å})$
	$\text{Gd}(\text{C}_4\text{F}_7\text{O}_2)_3 \cdot 3\text{H}_2\text{O}$
vs	14.25
vs	9.24
vs	7.73
vs	5.61
vs	4.62
m	4.39
m	4.20
m	4.01

Rel. intensity	$d(\text{Å})$		
	$\text{Ho}(\text{C}_4\text{F}_7\text{O}_2)_3 \cdot 2\text{H}_2\text{O}$	$\text{Er}(\text{C}_4\text{F}_7\text{O}_2)_3 \cdot 2\text{H}_2\text{O}$	$\text{Yb}(\text{C}_4\text{F}_7\text{O}_2)_3 \cdot 2\text{H}_2\text{O}$
vs	13.91	13.91	13.87
s	10.40	10.34	10.42
m	8.97	8.97	8.97
m	7.78	7.78	7.78
m	6.21	6.19	6.18
m	4.98	4.96	4.97
s	4.58	4.59	4.58
m	4.20	4.19	4.18
m	4.15	4.13	4.14
m	4.10	4.10	4.11
m	3.29	3.29	3.28

value. In that the TG values listed in Table 3 support these findings, no specific elemental data are reported. Further details can be found in ref. 6.

### Thermal analysis

Thermal methods were described in a previous paper<sup>2</sup> with the following exception. The high temperature DTA cell was replaced by the Dupont Model 900 DSC cell. The DSC experiments were run in a qualitative sense to overcome baseline difficulties arising from the high temperature DTA cell. The heating rate was  $10^{\circ}\text{C min}^{-1}$  and except where indicated, the atmosphere was flowing dried air ( $60\text{ ml min}^{-1}$ ). The reference and sample pans were constructed of platinum and shaped like a shallow "cupcake" each weighing 0.10 g. Sample sizes were approximately 10 mg and were run against an air reference. Ordinate sensitivity varied and is indicated on all curves. The abscissa was displayed as degrees centigrade.

Analytical, powder X-ray diffraction and infrared methods were described in a previous paper<sup>2</sup>.

### RESULTS AND DISCUSSION

Results of the hydration studies revealed the rare earth heptafluorobutyrate to show several different hydration states (Table 1). The extent of hydration for these compounds was found to decrease gradually with an increase in atomic number. Powder X-ray diffraction data revealed the salts to exist in three different crystalline structures. By virtue of similar  $d$  values and line intensities (Table 2), Pr, Sm and Eu are considered isomorphous and belong to the first crystal group. The Gd salt,

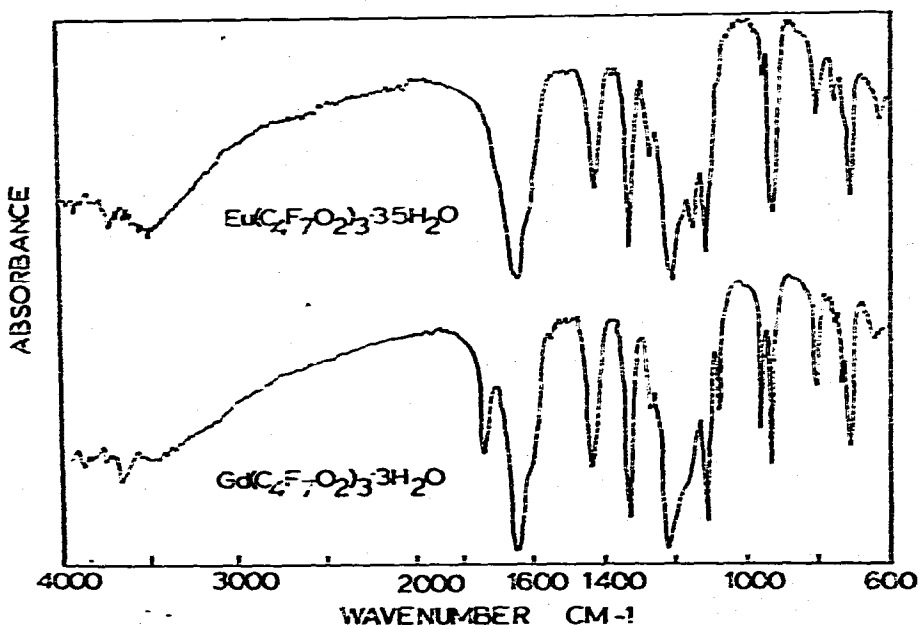


Fig. 1. Infrared spectra of  $\text{Eu}(\text{C}_4\text{F}_7\text{O}_2)_3 \cdot 3.5\text{H}_2\text{O}$  and  $\text{Gd}(\text{C}_4\text{F}_7\text{O}_2)_3 \cdot 3\text{H}_2\text{O}$ .

belonging to the second crystal structure, is different from any of the other members in that the powder pattern contained five very strong lines having considerably different  $d$  values from the others. Ho, Er and Yb were found to be isomorphous and belong to the third crystalline group. The hydration data agree well with the X-ray results in that the reported hydration states fall into the same groupings as those suggested by diffraction data.

Infrared spectra suggested two structural arrangements as shown by typical spectra for  $\text{Eu}(\text{C}_4\text{F}_7\text{O}_2)_3 \cdot 3.5 \text{H}_2\text{O}$  and  $\text{Gd}(\text{C}_4\text{F}_7\text{O}_2)_3 \cdot 3 \text{H}_2\text{O}$  (Fig. 1). The spectrum for the Eu compound is typical of the Pr and Sm compounds while the Gd spectrum is similar to the Ho, Er, Yb compounds. These findings are in agreement with the above hydration data and X-ray results, the only exception being that two types of structures are indicated by the infrared analysis while three distinct structures were observed by means of X-ray diffraction and hydration studies. The major differences between the two infrared spectra lie in the splitting of the asym.  $\text{COO}^-$  band (approximately  $1655 \text{ cm}^{-1}$ ). Spectra for the Pr, Sm, and Eu compounds showed one broad asym.  $\text{COO}^-$  band while those of Gd, Ho, Er and Yb revealed a distinct splitting of the asym.  $\text{COO}^-$  band as shown in Fig. 1. Other differences between the two groups are the intensity changes for the bands at  $945$ ,  $1093$  and  $1279 \text{ cm}^{-1}$ .

Russian workers<sup>3</sup> found similar splitting of both asym. and sym.  $\text{COO}^-$  bands for a series of lanthanide acetates. These workers suggested that the splitting resulted from the interaction of the anions coordinated with one and the same cation. Studies by Karraher<sup>4</sup> also revealed  $\text{COO}^-$  band splitting for rare earth acetates. Karraher suggested the band splitting to arise from complex metal acetate bonding of the polymeric type involving both metal-oxygen and metal-oxygen-metal interaction.

Upon partial dehydration of the Pr, Sm and Eu salts, the infrared spectra revealed the asym.  $\text{COO}^-$  band to split showing a close similarity to the heavier members. The  $\text{Eu}(\text{C}_4\text{F}_7\text{O}_2)_3 \cdot 3.5 \text{H}_2\text{O}$  compound was dehydrated to  $\text{Eu}(\text{C}_4\text{F}_7\text{O}_2)_3 \cdot 2\text{H}_2\text{O}$  by means of the thermal balance and subjected to powder X-ray diffraction studies. Similar crystal structures were observed for the  $\text{Eu}(\text{C}_4\text{F}_7\text{O}_2)_3 \cdot 2 \text{H}_2\text{O}$  and the Ho, Er, Yb dihydrates. Further dehydration of the Eu compound and a dihydrated Ho salt to the anhydrous state and subsequent X-ray examination revealed no further structural changes.

Nakamoto et al.<sup>5</sup> were able to distinguish between monodentate and bidentate structures of  $\text{Ni}(\text{ac})_2 \cdot 4 \text{H}_2\text{O}$  and  $\text{Cu}_2(\text{ac})_4 \cdot 2 \text{H}_2\text{O}$  by means of the frequency difference between the asym. and sym.  $\text{COO}^-$  stretching vibrations. Application of this method revealed the frequency differences for the salts of this study to be  $217\text{--}220 \text{ cm}^{-1}$  for the Pr, Sm and Eu compounds and  $200\text{--}205 \text{ cm}^{-1}$  for the Gd, Ho, Er, Yb salts. These data suggest two types of coordination and agree well with previous findings. Dehydration of the Eu and Pr compounds to the dihydrate revealed a change of the  $\Delta\nu$  values from  $217\text{--}220 \text{ cm}^{-1}$  to  $205 \text{ cm}^{-1}$ . The latter value is identical to that found for the Gd, Ho, Er and Yb compounds. It appears that the extra water molecules in the Pr, Sm and Eu compounds play a key role in the coordination and crystal structures of these compounds. Upon removal of 2 and 1.5 moles of water to

obtain the dihydrates, the compounds go through a structural change and become similar to the dihydrates of the heavy series. It seems reasonable that the higher hydration states obtained by the lighter series may reflect the differences in the size of the ionic radius. The lighter series having the larger radius may accommodate the extra water molecules more easily.

Thermogravimetric studies revealed the decomposition to proceed in a manner similar to that previously reported<sup>2</sup> for trifluoroacetates and pentafluoropropionates.

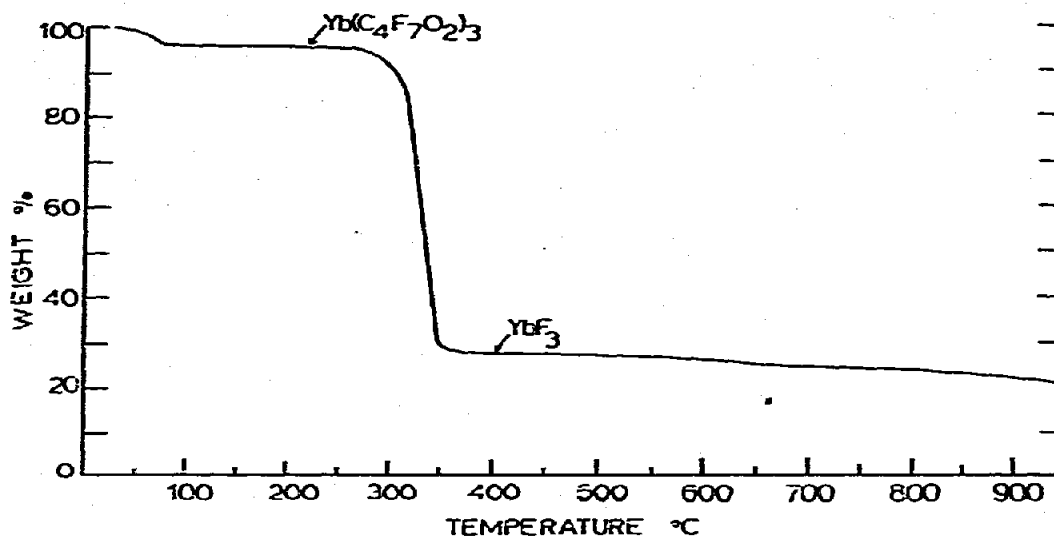


Fig. 2. Thermogravimetric curve for  $\text{Yb}(\text{C}_4\text{F}_7\text{O}_2)_3 \cdot 2\text{H}_2\text{O}$  in air at atmospheric pressure.

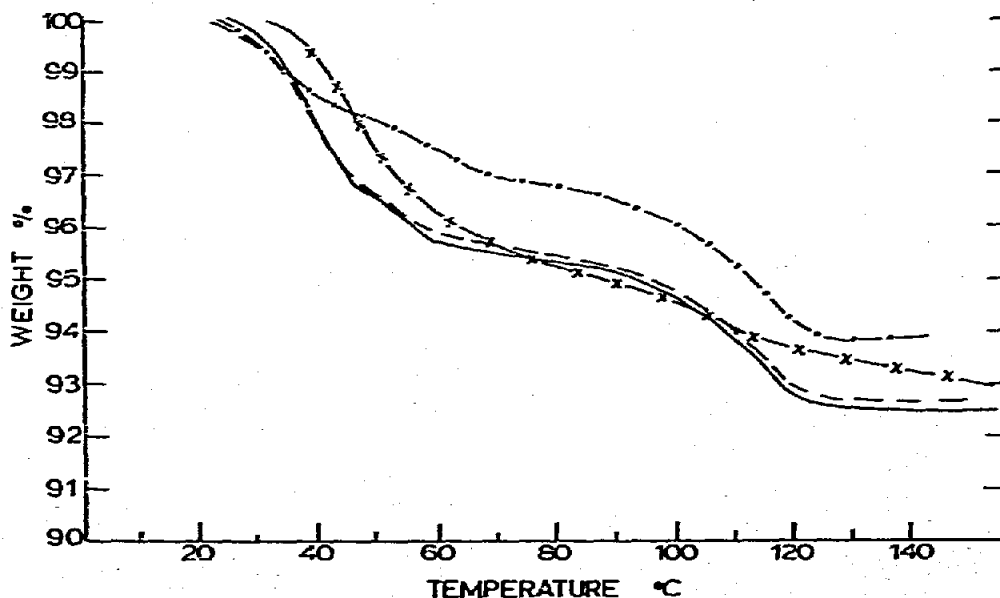


Fig. 3. Dehydration thermogravimetric curves. x-x,  $\text{Pr}(\text{C}_4\text{F}_7\text{O}_2)_3 \cdot 4\text{H}_2\text{O}$ ; ---,  $\text{Sm}(\text{C}_4\text{F}_7\text{O}_2)_3 \cdot 3.5\text{H}_2\text{O}$ ; —,  $\text{Eu}(\text{C}_4\text{F}_7\text{O}_2)_3 \cdot 3.5\text{H}_2\text{O}$ ; - - - -,  $\text{Gd}(\text{C}_4\text{F}_7\text{O}_2)_3 \cdot 3\text{H}_2\text{O}$ .

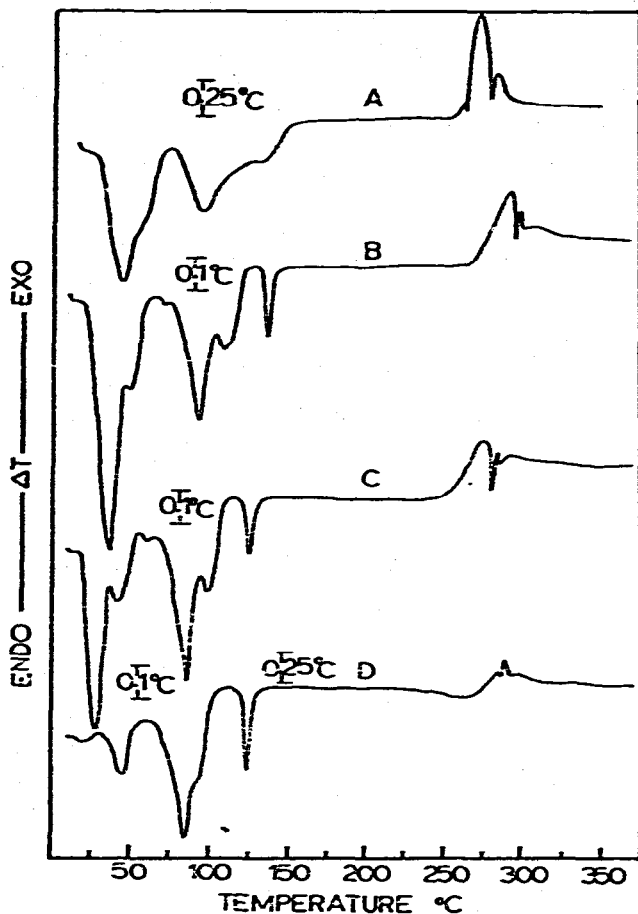


Fig. 4. DSC curves. (A)  $\text{Pr}(\text{C}_4\text{F}_7\text{O}_2)_3 \cdot 4\text{H}_2\text{O}$ ; (B)  $\text{Sm}(\text{C}_4\text{F}_7\text{O}_2)_3 \cdot 3.5\text{H}_2\text{O}$ ; (C)  $\text{Eu}(\text{C}_4\text{F}_7\text{O}_2)_3 \cdot 3.5\text{H}_2\text{O}$ ; (D)  $\text{Gd}(\text{C}_4\text{F}_7\text{O}_2)_3 \cdot 3\text{H}_2\text{O}$ .

The first stage of decomposition involved a stepwise dehydration to the anhydrous state, followed by rapid decomposition of the salt to a stable product. Subsequent decomposition of this product comprised the final stage. In all cases the compounds decomposed to the  $\text{LnF}_3$  product as shown in Fig. 2. Upon further heating in an air atmosphere, slow decomposition took place resulting in  $\text{LnOF}$ . Under hydrolyzing conditions (air atmosphere saturated with water) and additional heat  $\text{Ln}_2\text{O}_3$  was formed. All of the above products were confirmed by powder X-ray diffraction studies. Further details can be found in refs. 2 and 6.

#### $\text{Pr}(\text{C}_4\text{F}_7\text{O}_2)_3 \cdot 4\text{H}_2\text{O}$ (Fig. 3)

This compound began to lose hydrate water at  $35^\circ\text{C}$  giving two poorly defined breaks prior to reaching the anhydrous state. The first break occurred at  $70^\circ\text{C}$  and corresponded to the dihydrate. The dihydrate immediately dehydrated to the monohydrate which appeared as the second break on the TG curve at  $116^\circ\text{C}$ . Neither of the above intermediates showed any degree of stability. Slow dehydration followed,

finally reaching the anhydrous state at 160°C. The anhydrous compound was stable from 160°C to approximately 250°C after which decomposition took place resulting in  $\text{PrF}_3$ .

The DSC curve (Figure 4) for this compound revealed a strong endotherm beginning at 30°C and peaking at 45°C which corresponded to the loss of two moles of water. A shoulder peak on this strong endotherm at 55°C and returning to the baseline at 75°C is most likely associated with the loss of an additional mole of water to form the monohydrate. A second endotherm beginning at 75°C and peaking at 92°C followed by a very gradual return to baseline corresponds to the gradual loss of the last mole of hydrate water. A hot stage microscopy study of this compound revealed the crystals to go gradually into solution over a temperature range of 110 to 150°C. It is assumed that the solution, observed during the microscopy studies, is not a result of melting but a result of the anhydrous compound dissolving in its own evolved water of hydration. A lack of reversibility of the DSC endotherm supports this conclusion. The shallow endotherm at 125°C is probably associated with the observed solution effect. Decomposition took place in what appeared to be a three step process. No indication of a multistage decomposition was observed in the TG studies. Most likely the multistage decomposition was not resolved in the TG curve due to the exothermic reaction taking place. In most cases the large evolution of heat was enough to temporarily override the temperature programmer of the TG unit which resulted in a slightly skewed curve. The peak temperature for the largest of the three exotherms appeared at 272°C. The decomposition of this compound was considerably less exothermic than the previously reported<sup>2</sup> trifluoroacetates and pentafluoropropionates.

#### $\text{Sm}(\text{C}_4\text{F}_7\text{O}_2)_3 \cdot 3.5 \text{H}_2\text{O}$ (Fig. 3)

Hydrate water began to evolve at 25°C giving two breaks before reaching the anhydrous condition. The first break at 45°C corresponded to the dihydrate. Further dehydration with the loss of 0.5 moles of water resulted in the second break at 60°C giving the 1.5 hydrate. The anhydrous state was reached at 124°C with an additional loss of 1.5 moles of water. The weight loss curve was not smooth and may indicate that another very unstable intermediate was formed prior to reaching the anhydrous condition. The anhydrous compound was stable over a temperature range of 100°C.

The DSC curve (Fig. 4) revealed a strong endotherm with a peak temperature of 35°C which corresponds to the loss of 1.5 moles of water. A shoulder peak on the main endotherm appears at 45°C and is most likely the endothermic effect from the loss of 0.5 moles of hydrate water. Two additional endotherms appear at 90 and 110°C with the former having approximately twice the intensity of the latter. It appears that these endotherms are a result of the dehydration of the remaining 1.5 moles of water in which first one mole of water is lost followed immediately by loss of an additional 0.5 mole of water. This two step process was not resolved adequately to be recognized in the TG curve. An alternate explanation may describe the first large endotherm at 90°C to result from dissociation of 1.5 moles of water



and then vaporization of the same at 110°C. Electrical conductivity experiments described by Wendlandt<sup>7</sup> would be required to resolve this possibility. Microscopic examination of this compound revealed the crystals to remain solid up to the decomposition temperature. However, the crystals were observed to become wet in the temperature range of 75 to 100°C indicating some absorption of evolved water. The weak peak at 75°C might result from the absorption of the water. The sharp endotherm at 133°C was found to be reversible. Microscopy studies did not reveal any obvious phase changes; however, many times phase changes are not detectable by this method. Heating the compound at temperatures of 125 to 150°C revealed the crystals to become tacky without any loss of shape. Upon cooling, the compound returned to its original state. It appears that this reversible peak is a temperature dependent phase change which would be detectable by an elevated temperature X-ray study. Decomposition was exothermic and went through a three step process. The peak temperature for the largest of the three exotherms appeared at 285°C.

*Eu(C<sub>4</sub>F<sub>7</sub>O<sub>2</sub>)<sub>3</sub> · 3.5 H<sub>2</sub>O (Fig. 3)*

This compound was very similar thermally to the samarium compound. Hydrate water began to evolve at 25°C giving two breaks before reaching the anhydrous state. The first break at 46°C corresponded to the dihydrate. The second break in the curve at 58°C was due to the loss of an additional 0.5 mole of water. Further dehydration resulted in the loss of 1.5 moles of water and the formation of the anhydrous compound at 120°C. The anhydrous compound was stable over a 120°C temperature range.

The DSC curve (Fig. 4) shows a large endotherm from the loss of 1.5 moles of

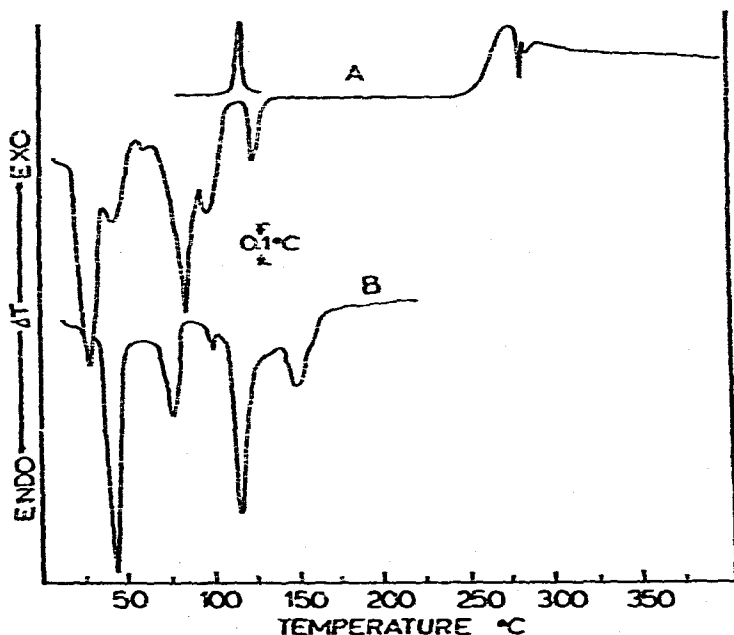


Fig. 5. DSC curves for  $\text{Eu}(\text{C}_4\text{F}_7\text{O}_2)_3 \cdot 3.5\text{H}_2\text{O}$ . (A) flowing air atmosphere; (B) static air atmosphere.

water with a peak temperature of 27°C and a shoulder peak from the loss of 0.5 mole of water peaking at 43°C. As in the case of the samarium compound the dehydration of the remaining 1.5 moles of water occurs in two steps which appear to go in steps of 1 mole of water and 0.5 mole of water. The alternate explanation for the Sm compound given above may also apply. The above results were obtained in a flowing air atmosphere. In an effort to resolve the shoulder peaks more completely the sample was rerun under static conditions (1 atm pressure). Figure 5 illustrates the effect of the static atmosphere on the dehydration endotherms. The fact that the shoulder peaks were shifted with increased resolution adds support to the assignment of these peaks as dehydration endotherms. It was shown previously<sup>2</sup> that a wet atmosphere enhances the resolution of intermediate hydrates on the TG curve. The reversible peak was not shifted nearly as much, resulting in superposition of the last dehydration endotherm. Since the reversible peak is not dependent on the vapor pressure of water, it is reasonable that a smaller temperature shift took place. The reversibility of this transition is also illustrated in the top curve of Fig. 5. The reversible peak appears at 123°C. Decomposition took place in a three step process with the largest of the three exotherms appearing at 275°C.

*Gd(C<sub>4</sub>F<sub>7</sub>O<sub>2</sub>)<sub>3</sub> · 3 H<sub>2</sub>O (Fig. 3)*

The compound began to lose hydrate water at 25°C giving two breaks in the TG curve prior to reaching the anhydrous state. The first break at 50°C corresponded to the loss of one mole of water with the resultant formation of the dihydrate. The second break at 70°C corresponds to an additional loss of 0.5 mole of water to give the 1.5 hydrate. Further dehydration resulted in the loss of the remaining 1.5 moles

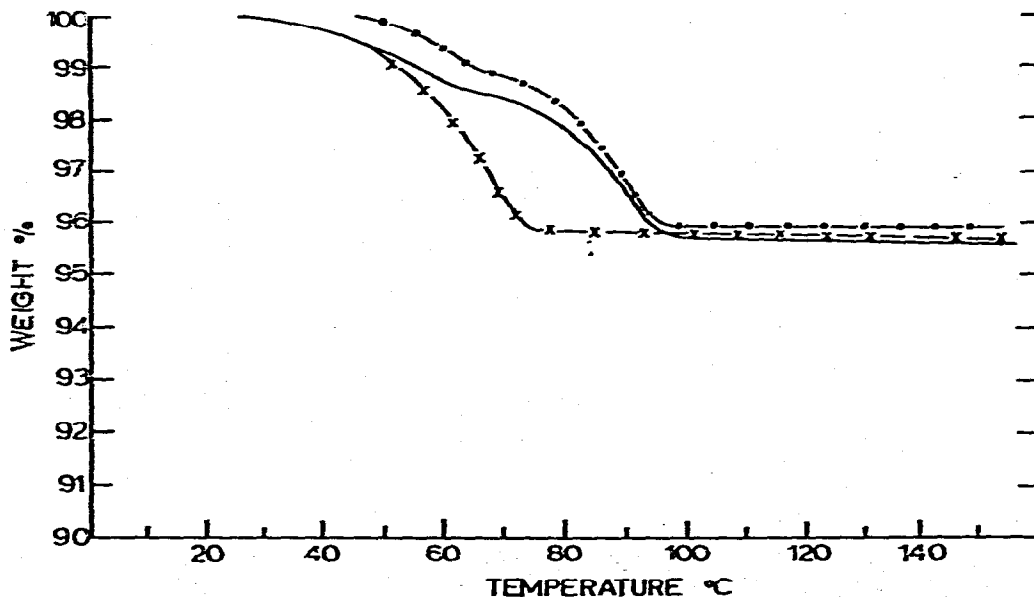


Fig. 6. Dehydration thermogravimetric curves. —, Ho(C<sub>4</sub>F<sub>7</sub>O<sub>2</sub>)<sub>3</sub> · 2H<sub>2</sub>O; - - -, Er(C<sub>4</sub>F<sub>7</sub>O<sub>2</sub>)<sub>3</sub> · 2H<sub>2</sub>O.

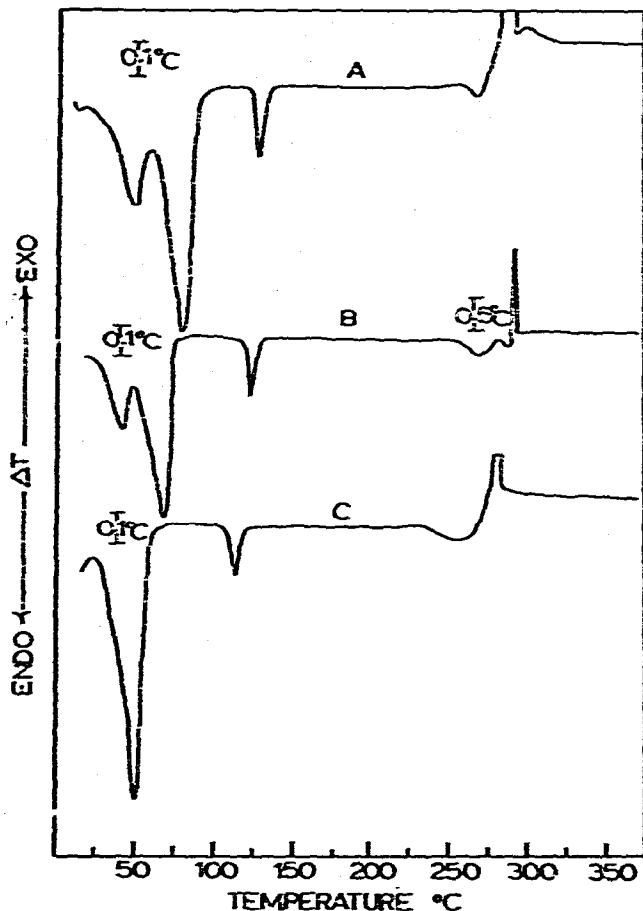


Fig. 7. DSC curves. (A)  $\text{Ho}(\text{C}_4\text{F}_7\text{O}_2)_3 \cdot 2\text{H}_2\text{O}$ ; (B)  $\text{Er}(\text{C}_4\text{F}_7\text{O}_2)_3 \cdot 2\text{H}_2\text{O}$ ; (C)  $\text{Yb}(\text{C}_4\text{F}_7\text{O}_2)_3 \cdot 2\text{H}_2\text{O}$ .

of water which appeared to take place in a one step process giving the anhydrous compound at a temperature of  $124^\circ\text{C}$ . The anhydrous compound was stable over a temperature range of  $120^\circ\text{C}$ .

The DSC curve (Fig. 4) shows one strong endotherm at  $45^\circ\text{C}$  preceded by a weak endotherm at approximately  $20^\circ\text{C}$  of unknown origin. The strong endotherm is probably associated with the loss of one mole of water. A second endotherm is complex and appears to have a shoulder peak on each side of the main endotherm. The first shoulder starting at approximately  $65^\circ\text{C}$  and ranging to  $80^\circ\text{C}$  is probably associated with the loss of the additional 0.5 mole of water. The main endotherm at  $90^\circ\text{C}$  and its shoulder peak at  $97^\circ\text{C}$  may indicate that the loss of its final 1.5 moles of water takes place in a two step process of 1 mole of water immediately followed by loss of 0.5 mole of water. As with the Sm and Eu compounds the shoulder at  $97^\circ\text{C}$  may also be vaporization of the dissociated 1.5 moles of water. The reversible peak noted in the previous compounds appears at  $123^\circ\text{C}$ . Decomposition takes place in a three step exothermic process with a peak temperature of  $285^\circ\text{C}$ ; however, prior to

the exothermic decomposition, a broad shallow endothermic peak appeared at approximately 225°C. This was not found for the Pr, Sm, and Eu compounds.

*Ho(C<sub>4</sub>F<sub>7</sub>O<sub>2</sub>)<sub>3</sub> · 2 H<sub>2</sub>O (Fig. 6)*

Dehydration began at 30°C giving one break in the TG curve prior to reaching the anhydrous state. The first break at 60°C corresponded to the loss of 0.5 mole of water followed by dehydration of the remaining 1.5 moles of water to the anhydrous state at 98°C. The anhydrous compound was stable over a temperature range of 145°C.

The DSC curve (Fig. 7) was much less complex than the lighter group compounds in that only three endotherms were present. The first endotherm reached a peak temperature at 47°C and corresponded to the loss of 0.5 mole of water. The second endotherm began at 60°C and reached a peak temperature at 80°C. Both the temperature and magnitude of this endotherm indicate it is due to the loss of 1.5 moles of water. The reversible peak is sharp and appears at a temperature of 125°C. The decomposition took place in three stages with the maximum exothermic peak having a temperature of 285°C. As noted in the curve for the Gd compound an endothermic peak at 265°C preceded the exotherm.

*Er(C<sub>4</sub>F<sub>7</sub>O<sub>2</sub>)<sub>3</sub> · 2 H<sub>2</sub>O (Fig. 6)*

The erbium compound was very similar to the holmium compound in that hydration water began to evolve at 40°C giving one break in the TG curve prior to reaching the anhydrous compound. The first break at 64°C corresponded to the loss of 0.5 mole of water giving the 1.5 hydrate. The remaining 1.5 moles of water were lost in a one step process resulting in the formation of the anhydrous compound at 96°C. The anhydrous compound was stable over a temperature range of 160°C.

The DSC curve (Fig. 7) revealed three endothermic peaks having a pattern identical to the previously described holmium compound. The first endotherm had a peak temperature of 45°C and corresponded to the loss of 0.5 mole of water. The second endotherm corresponded to the loss of the remaining 1.5 moles of water. The reversible peak appeared at 120°C. The decomposition proceeded much the same way as the previous compound in that an endothermic peak at 260°C preceded a three step exothermic decomposition. The peak temperature of the largest exotherm appeared at 290°C.

*Yb(C<sub>4</sub>F<sub>7</sub>O<sub>2</sub>)<sub>3</sub> · 2 H<sub>2</sub>O (Fig. 6)*

This compound showed the least complexity of all the compounds investigated. Hydrate water began to evolve at 25°C and continued, losing two moles of water in a one step process. The anhydrous compound was reached at 72°C and was found to be stable over a temperature range of 165°C.

The DSC curve (Figure 7) showed only one strong endotherm having a peak temperature of 50°C. The peak corresponded to the one step loss of the two moles

of hydrate water. The reversible peak appeared at 110°C. A broad shallow endotherm at 255°C preceded the three step exothermic decomposition.

Anhydrous praseodymium and erbium heptafluorobutyrate were heated in a vacuum (5–10 u Hg) at temperatures of 300, 350 and 500°C. At a pyrolysis temperature of 300°C, the evolved gases were identified by infrared analysis and found to consist of carbon monoxide, carbon dioxide and a mixture of fluorinated compounds. The fluorinated mixture consisted of major amounts of pentafluoropropionyl fluoride and heptafluorobutyryl fluoride. A possible trace of heptafluorobutyric anhydride was also indicated. At a pyrolysis temperature of 350°C the concentration of carbon dioxide and carbon monoxide diminished along with the concentration of heptafluorobutyryl fluoride. Finally, at 500°C no significant amounts of carbon monoxide and carbon dioxide were present and only trace amounts of heptafluorobutyryl fluoride were found. The major product was pentafluoropropionyl fluoride. It appears that a carbon-to-carbon cleavage is taking place which is enhanced by higher temperatures. An interesting reaction reported by Steunenbergh and Cady<sup>8</sup> suggests that a number of saturated fluorocarbons may decompose by a process whereby a fluorine atom is transferred from one carbon to the next splitting off the remaining difluoromethylene group. Reactions such as the production of hexafluoroethane from octafluoropropane were reported in their study. The absence of carbonyl difluoride in the decomposition products of the heptafluorobutyrate suggests a different mechanism of decomposition from that previously reported<sup>2</sup> for trifluoroacetates. In the latter case a considerable amount of carbonyl difluoride was found in the decomposition products.

Previously reported<sup>2</sup> thermal studies of pentafluoropropionates revealed their dehydration to proceed to a 1.5 hydrate intermediate before reaching the anhydrous state. In this study, it appears that the 2.0 hydrate is preferred as the decomposition intermediate for the cerium group compounds while the yttrium series is stable at room temperature as the dihydrates. Upon reaching the dihydrate intermediate, the cerium group compounds dehydrate to the anhydrous state in an identical manner to that revealed for the yttrium series compounds. These findings are supported by the infrared and X-ray studies in that the infrared spectra of the cerium group compounds became similar to the yttrium series upon dehydration to the dihydrate. Also, the dihydrated cerium compounds showed identical X-ray patterns to the yttrium dihydrates.

All of the anhydrous salts of the heptafluorobutyrate were stable over a range of temperatures as indicated by a level plateau on the TG curve. These findings differ slightly with the trifluoroacetates and pentafluoropropionates in that the praseodymium and samarium salts of the trifluoroacetates and the praseodymium salt of the pentafluoropropionates were unstable. A trend was indicated in that the stability of the anhydrous compounds increased as the atomic number increased as shown by the increasing procedural decomposition temperatures in Table 3. This appears to be a direct result of the lanthanide contraction if looked upon from an electrostatic viewpoint since as the cation radius decreases the charge density increases, resulting

TABLE 3

TG DATA FOR HEPTAFLUOROBUTYRATES

Compound	Procedural decomposition temp. (°C)	Wt % as anhydrous		Wt % as LnF <sub>3</sub>		Wt % as LnOF		Temp. of LnOF formation (°C)
		Theory	Found	Theory	Found	Theory	Found	
Pr(C <sub>4</sub> F <sub>7</sub> O <sub>2</sub> ) <sub>3</sub> · 4H <sub>2</sub> O	298	91.7	92.0	23.3	23.8	20.7	21.0	670
Sm(C <sub>4</sub> F <sub>7</sub> O <sub>2</sub> ) <sub>3</sub> · 3.5H <sub>2</sub> O	303	92.5	92.2	24.3	24.5	21.7	21.8	650
Eu(C <sub>4</sub> F <sub>7</sub> O <sub>2</sub> ) <sub>3</sub> · 3.5H <sub>2</sub> O	304	92.5	92.5	24.5	25.0	21.9	22.0	630
Gd(C <sub>4</sub> F <sub>7</sub> O <sub>2</sub> ) <sub>3</sub> · 3H <sub>2</sub> O	309	93.7	94.0	25.2	25.5	22.6	22.9	625
Ho(C <sub>4</sub> F <sub>7</sub> O <sub>2</sub> ) <sub>3</sub> · 2H <sub>2</sub> O	314	95.7	95.6	26.4	26.6	23.8	24.0	610
Er(C <sub>4</sub> F <sub>7</sub> O <sub>2</sub> ) <sub>3</sub> · 2H <sub>2</sub> O	315	95.7	95.5	26.6	26.5	24.0	23.8	600
Yb(C <sub>4</sub> F <sub>7</sub> O <sub>2</sub> ) <sub>3</sub> · 2H <sub>2</sub> O	318	95.8	95.5	27.1	27.2	24.5	24.5	580

in a greater attraction for the ligands. Also, one could interpret these results from the base strengths of the respective elements with praseodymium being the most basic and ytterbium the least basic. It seems reasonable that a better electron acceptor would form a stronger bond with an electron donor, a situation which is found in the case of the heavier elements.

In comparison, the stability of the anhydrous salts of the three classes of compounds was observed to be in order of the most stable to least stable to be heptafluorobutyrate > pentafluoropropionate > trifluoroacetate. The order of stability appears to agree with the strengths of the three acids. All three are considered strong<sup>9</sup>; however, trifluoroacetic is the strongest with a dissociation constant of 1.8 and heptafluorobutyric ( $K_d = 1.1$ ) the weakest. Heptafluorobutyric acid being the weakest acid forms the most stable salts, while trifluoroacetic, the strongest acid, forms the least stable salts.

Qualitative estimates, from DSC measurements, revealed the trifluoroacetates to exhibit the most exothermic decomposition while the heptafluorobutyrate showed the least exothermic decompositions.

## REFERENCES

- 1 J. E. Roberts, *J. Am. Chem. Soc.*, 83 (1961) 1087.
- 2 K. W. Rillings and J. E. Roberts, *Thermochim. Acta*, 10 (1974) 285.
- 3 A. I. Grogorbev and V. N. Maksimov, *Russ. J. Inorg. Chem.*, 9 (1964) 580.
- 4 D. G. Karraher, *J. Inorg. Chem.*, 31 (1969) 2815.
- 5 K. Nakamoto, K. Fuyita, S. Tanaka and M. Kobajaski, *J. Am. Chem. Soc.*, 79 (1957) 4904.
- 6 K. W. Rillings, *Ph.D. Thesis*, University of Massachusetts, 1973.
- 7 W. W. Wendlandt, *Thermochim. Acta*, 1 (1970) 11.
- 8 R. K. Steunenberg and G. H. Cady, *J. Am. Chem. Soc.*, 74 (1952) 4165.
- 9 O. Redlich and G. C. Hood, *Discuss. Faraday Soc.*, 24 (1957) 83.